

**A rationally designed bifunctional oxygen electrocatalyst based on Co₂P
nanoparticles for Zn-air battery**

Qing Shi^{a,b}, Yapeng Zheng^b, Weijun Li^b, Bin Tang^a, Lin Qin^{*,a}, Weiyu Yang^b, Qiao Liu^{*,b}

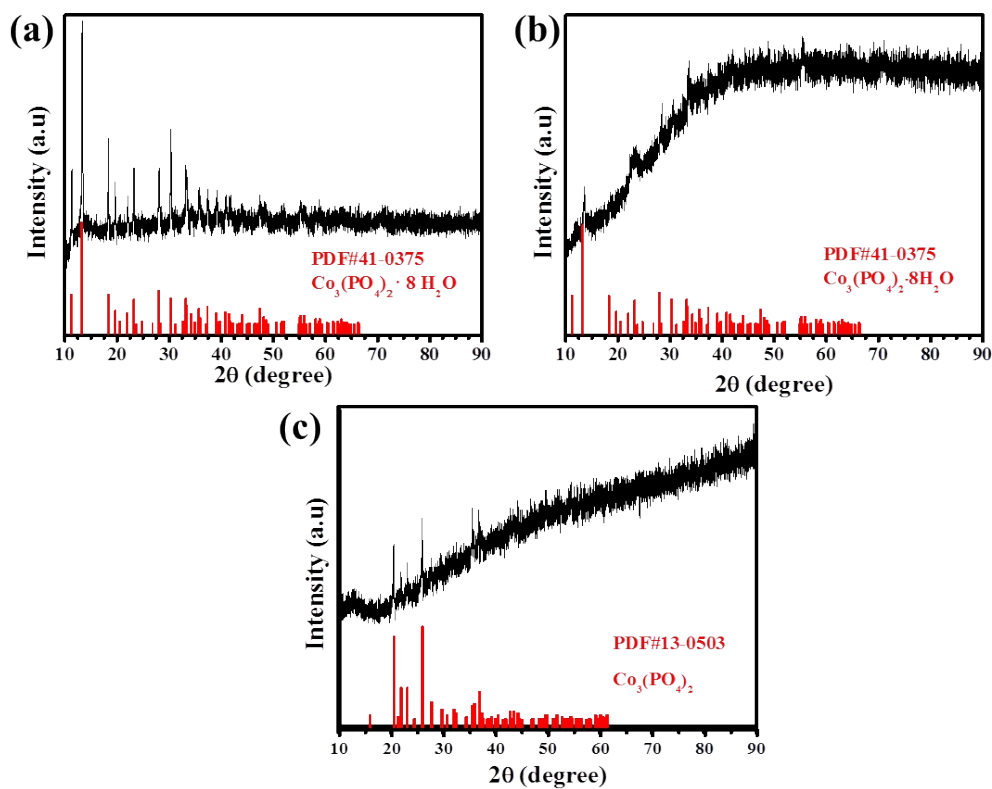


Fig. S1 Typical XRD patterns of intermediates: (a) $\text{Co}_3(\text{PO}_4)_2 \cdot 8\text{H}_2\text{O}$, (b) $\text{Co}_3(\text{PO}_4)_2 \cdot 8\text{H}_2\text{O}/\text{PDA}/\text{BC}$, (c) $\text{Co}_3(\text{PO}_4)_2$.

The sample of $\text{Co}_3(\text{PO}_4)_2 \cdot 8\text{H}_2\text{O}$ was prepared via the following procedure: First, adding 25 mL of Na_2HPO_4 (0.4 M) solution into 300 mL of DI water, then 10 mL of CoCl_2 solution (24 mg mL^{-1}) was added into the above mixture that kept stirring for 12 h; finally, the solids were collected by centrifuging, washing and freeze-drying.

The sample of $\text{Co}_3(\text{PO}_4)_2 \cdot 8\text{H}_2\text{O}/\text{PDA}/\text{BC}$ is the precursor of $\text{Co}_2\text{P-NPC}/\text{CF}$, and the sample of $\text{Co}_3(\text{PO}_4)_2$ is product of pyrolysis $\text{Co}_3(\text{PO}_4)_2 \cdot 8\text{H}_2\text{O}$ under Ar atmosphere at $900 \text{ }^\circ\text{C}$ for 3 h.

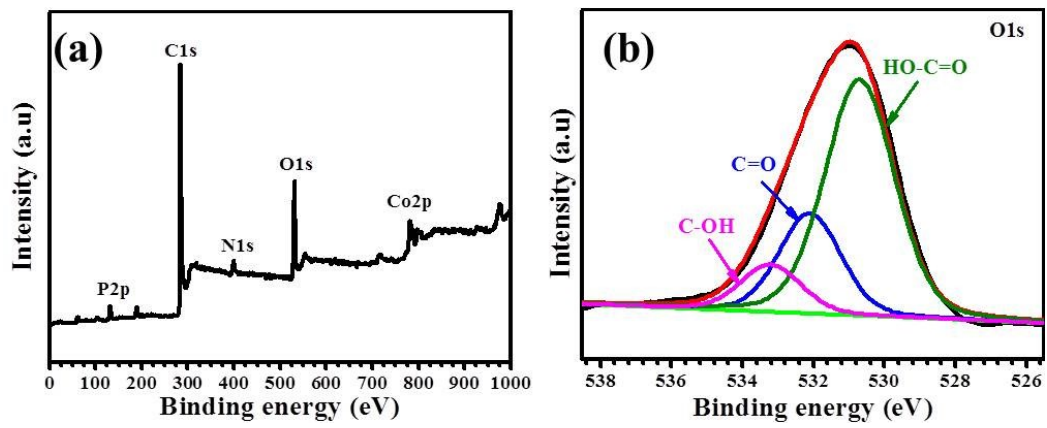


Fig. S2 (a) The XPS survey spectrum and (b) high-resolution O 1s spectrum of Co₂P-NPC/CF.

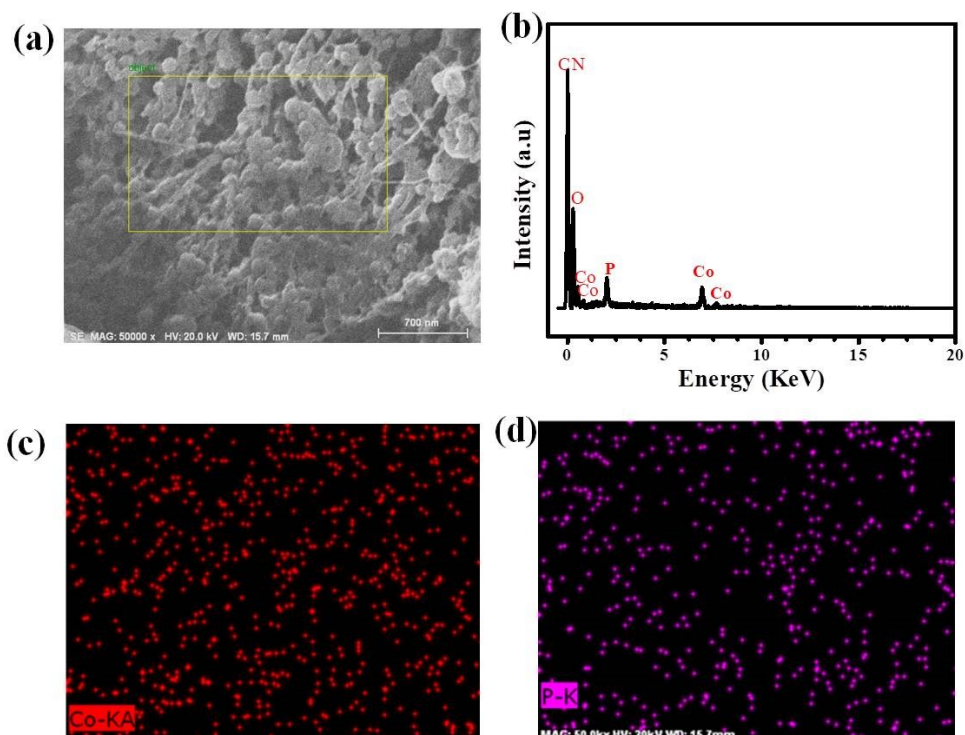


Figure S3 (a) SEM image and (b) EDS spectrum of $\text{Co}_3(\text{PO}_4)_2 \cdot 8\text{H}_2\text{O}/\text{PDA}/\text{BC}$.

In order to probe the P source for the doping of resultant carbon, the sample of $\text{Co}_3(\text{PO}_4)_2 \cdot 8\text{H}_2\text{O}/\text{PDA}/\text{BC}$ was investigated by EDS test. If the phosphorus source for the doping of carbon comes from Na_2HPO_4 , the $\text{Co}_3(\text{PO}_4)_2 \cdot 8\text{H}_2\text{O}/\text{PDA}/\text{BC}$ sample should contain a large number of adsorbed Na^+ and HPO_4^{2-} ions. In fact, before the pyrolysis transformation, $\text{Co}_3(\text{PO}_4)_2 \cdot 8\text{H}_2\text{O}/\text{PDA}/\text{BC}$ underwent the repetitive rinsing by deionized water, and the soluble species adsorbed in PDA/BC matrix can be completely removed. EDS spectrum shown in Figure S3b supports this assumption, where the Na^+ signal is absent, which suggests that the excessive Na_2HPO_4 has been washed away from $\text{Co}_3(\text{PO}_4)_2 \cdot 8\text{H}_2\text{O}/\text{PDA}/\text{BC}$.

To further determine whether there is residual HPO_4^{2-} adsorbant, we have also carried out elemental mapping on this sample, as shown in Figure S3c-d. It is found that the elemental distribution of P is not more scattered but almost the same as that of Co, indicating that the main form of existed P atoms lies in $\text{Co}_3(\text{PO}_4)_2$ rather than

adsorbed HPO_4^{2-} ions on PDA and/or BC. Therefore, it can be concluded that the major contributor of P doping in carbon comes from phosphorus in $\text{Co}_3(\text{PO}_4)_2$.

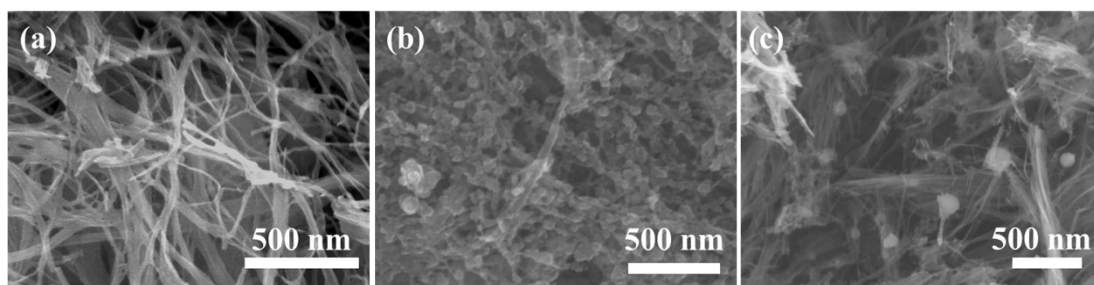


Fig. S4 The SEM images of as-fabricated materials: (a) CF, (b) NC/CF, and (c) Co₂P/CF.

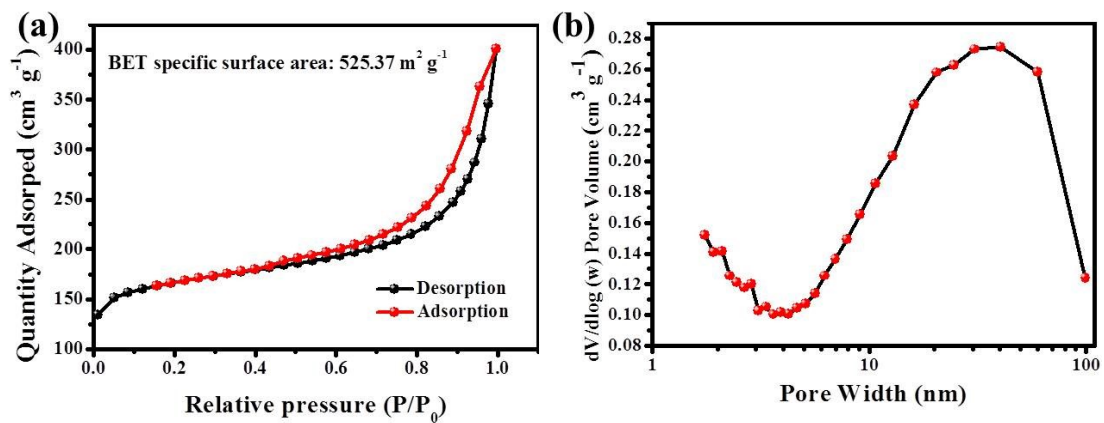


Fig. S5 (a) N₂ adsorption-desorption isotherm and (b) pore size distribution of Co₂P-NPC/CF.

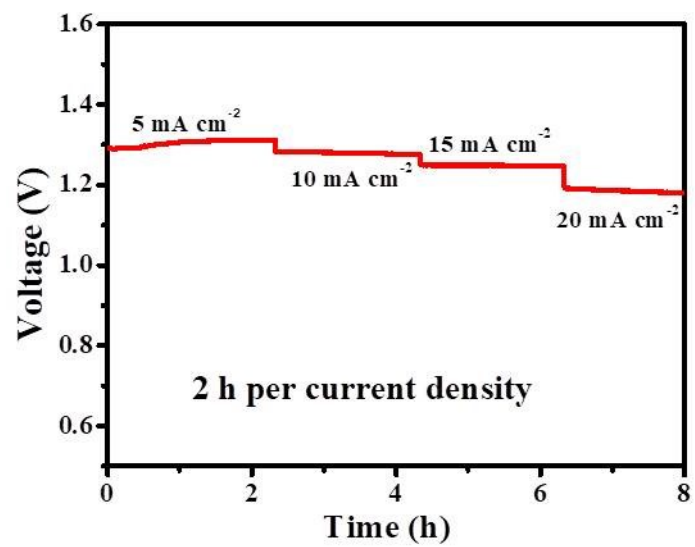


Fig. S6 Rate capability of Co₂P-NPC/CF

Table S1 The ORR performance of the as-fabricated materials and commercial Pt/C.

| Catalysts | E_{onset} (V) | $E_{1/2}$ (V) | Tafel slope (mV dec⁻¹) |
|-------------------------------|--|---------------------------------|--|
| CF | 0.66 | 0.51 | 102 |
| NC/CF | 0.85 | 0.64 | 90 |
| Co ₂ P/CF | 0.78 | 0.70 | 88 |
| Co₂P-NPC/CF | 0.94 | 0.85 | 52 |
| Pt/C | 0.95 | 0.82 | 80 |

Table S2 Overview of bifunctional activity of recently reported Co-containing carbon electrocatalysts towards ORR and OER in 0.1 M KOH.

| Catalysts | $E_{j=10}$ (V vs. RHE) | $E_{1/2}$ (V vs. RHE) | ΔE (V) | Ref. |
|--------------------------------|------------------------|-----------------------|----------------|------------------|
| Co ₂ P@CoNPG | 1.73 | 0.81 | 0.92 | 1 |
| NC@Co-NGC | 1.64 | 0.82 | 0.82 | 2 |
| CoNC@GF | 1.66 | 0.87 | 0.79 | 3 |
| Co ₂ P/CoN-in-NCNTs | 1.65 | 0.85 | 0.80 | 4 |
| CoPNi-N/C | 1.63 | 0.81 | 0.79 | 5 |
| CoFe/N-GCT | 1.67 | 0.79 | 0.88 | 6 |
| Co-NC@CoP-NC | 1.56 | 0.78 | 0.78 | 7 |
| CoNP@NC/NG | 1.62 | 0.78 | 0.84 | 8 |
| Co ₂ P@CNF | 1.69 | 0.803 | 0.887 | 9 |
| Cu-Co ₂ P@2D-NPC | 1.57 | 0.835 | 0.735 | 10 |
| Co₂P-NPC/CF | 1.59 | 0.85 | 0.75 | This work |

Table S3 The OER performance of the as-fabricated materials and commercial RuO₂.

| Catalysts | E_{j10} (V) | Tafel slope (mV dec ⁻¹) | R_{ct} (Ω) |
|-------------------------------|---------------|-------------------------------------|-----------------------|
| CF | Not reach | 110 | 183.7 |
| NC/CF | 1.69 | 99 | 96 |
| Co ₂ P/CF | 1.63 | 93 | 42.6 |
| Co₂P-NPC/CF | 1.60 | 66 | 17.7 |
| RuO ₂ | 1.62 | 83 | 23.4 |

Reference

- [1] H. Jiang, C. Li, H. Shen, Y. Liu, W. Li, J. Li, *Electrochim. Acta*, 2017, 231, 344-353.
- [2] S. Liu, Z. Wang, S. Zhou, F. Yu, M. Yu, C.Y. Chiang, W. Zhou, J. Zhao, J. Qiu, *Adv. Mater.*, 2017, 29, 201700874- 201700884.
- [3] S. Liu, M. Wang, X. Sun, N. Xu, J. Liu, Y. Wang, T. Qian, C. Yan, *Adv. Mater.*, 2018, 30, 201704898-201704906.
- [4] Y. Guo, P. Yuan, J. Zhang, H. Xia, F. Cheng, M. Zhou, J. Li, Y. Qiao, S. Mu, Q. Xu, *Adv. Funct. Mater.*, 2018, 28, 1805641.
- [5] Z. Li, H. He, H. Cao, S. Sun, W. Diao, D. Gao, P. Lu, S. Zhang, Z. Guo, M. Li, R. Liu, D. Ren, C. Liu, Y. Zhang, Z. Yang, J. Jiang, G. Zhang, *Appl. Catal. B: Environmental*, 2019, 240, 112-121.
- [6] X. Liu, L. Wang, P. Yu, C. Tian, F. Sun, J. Ma, W. Li, H. Fu, *Angew. Chem. Int. Edit*, 2018, 57, 16166-16170.
- [7] X. Li, Q. Jiang, S. Dou, L. Deng, J. Huo, S. Wang, *J. Mater. Chem. A.*, 2016, 4, 15836-15840.
- [8] X. Zhong, Y. Jiang, X. Chen, L. Wang, G. Zhuang, X. Li, J.-G., *J. Mater. Chem. A.*, 2016, 4, 10575-10584.
- [9] J. Gao, J. Wang, L. Zhou, X. Cai, D. Zhan, M. Hou, L. Lai, *ACS Appl. Mater. Interfaces*, 2019, 11, 10364-10372.
- [10] L. Diao, T. Yang, B. Chen, B. Zhang, N. Zhao, C. Shi, E. Liu, L. Ma, C. He, *J. Mater. Chem. A.*, 2019, 7, 21232-21243.